



Eidgenössische Technische Hochschule Zürich  
Swiss Federal Institute of Technology Zurich



## Smart single-chip gas sensor microsystem

C. Hagleitner, A. Hierlemann, D. Lange, A. Kummer, N. Kerness, O. Brand & H. Baltes

Physical Electronics Laboratory, ETH Zurich, Hönggerberg, HPT H 6, CH-8093 Zurich, Switzerland

Research activity in chemical gas sensing is currently directed towards the search for highly selective (bio)chemical layer materials, and to the design of arrays consisting of different partially selective sensors that permit subsequent pattern recognition and multi-component analysis<sup>1-3</sup>. Simultaneous use of various transduction platforms has been demonstrated<sup>4-6</sup>, and the rapid development of integrated-circuit technology has facilitated the fabrication of planar chemical sensors<sup>7,8</sup> and sensors based on three-dimensional microelectromechanical systems<sup>9,10</sup>. Complementary metal-oxide silicon processes have previously been used to develop gas sensors based on metal oxides<sup>11</sup> and acoustic-wave-based sensor devices<sup>12</sup>. Here we combine several of these developments to fabricate a smart single-chip chemical microsensor system that incorporates three different transducers (mass-sensitive, capacitive and calorimetric), all of which rely on sensitive polymeric layers to detect airborne volatile organic compounds. Full integration of the microelectronic and micromechanical components on one chip permits control and monitoring of the sensor functions, and enables on-chip signal amplification and conditioning that notably improves the overall sensor performance. The circuitry also includes analog-to-digital converters, and an on-chip interface to transmit the data to off-chip recording units. We expect that our approach will provide a basis for the further development and optimization of gas microsystems.

Physisorption and bulk dissolution of analyte molecules within the polymer volume constitute the predominant interaction mechanisms of polymer-based sensors<sup>13</sup>. The physical properties of the polymer change on absorption of analytes: in the system we report here, these changes are detected by three distinct complementary metal-oxide silicon (CMOS) microtransducers (Fig. 1) in response to fundamentally different molecular properties of the analytes. One transducer (Fig. 1b) responds to the mass of sorbed molecules, another responds to the heat of absorption (Fig. 1c), and the third—the capacitive sensor—responds to a combination of the volume and dielectric properties of the absorbates convoluted with changes in these parameters for the sensing layer (Fig. 1a).

The capacitive sensor relies on interdigitated electrode structures, which correspond to the two plates of a standard capacitor, to monitor changes of the dielectric coefficient of the polymer. One electrode is made of the first metal layer of the CMOS process (E2 in Fig. 1a), whereas the second electrode is a stack of two metal layers (E1 in Fig. 1a). This is to enhance the sensitivity of the capacitive microsystem by increasing the number of electric field lines within the polymer volume by applying a 'three-dimensional' design<sup>14</sup>. The dimensions of the capacitor are  $800 \times 800 \mu\text{m}$ , and its electrode width and spacing are  $1.6 \mu\text{m}$ . As the nominal capacitance of the interdigitated capacitor is a few picofarads, and the expected capacitance changes on absorption of a volatile organic compound are in the attofarad range, a dedicated on-chip measurement configuration and specific signal-conditioning circuitry had to be developed. The sensor response is read out as a differential signal between a polymer-coated sensing capacitor and a passivated reference capacitor. A digital output signal is then generated by comparing the minute loading currents of both capacitors using fully differential second-order sigma-delta modulator circuitry<sup>14</sup>. The final output is a digital word with a precision of 20 bits.

Within the capacitive sensor, the space containing 95% of the electric field includes a polymer volume that is within a distance from the transducer surface of half the periodicity of the electrodes. For a layer thickness of less than half the periodicity, swelling of the polymer on analyte absorption always results in a capacitance increase, regardless of the dielectric constant of the absorbed analyte. This is due to the increased polymer/analyte volume within the field-line region exhibiting a larger dielectric constant than that of the air it displaces. On the other hand, the capacitance change for a polymer layer thickness larger than half the periodicity of the electrodes is determined by the ratio of dielectric constants of analyte and polymer. If the dielectric constant of the polymer is lower than that of the analyte, the capacitance will be increased, and if the polymer dielectric constant is larger, the capacitance will be decreased. This effect has been previously detailed and supported by simulations<sup>15</sup>.

The second type of transducer is a micromachined cantilever, which has been developed in the context of atomic force microscopy<sup>16–19</sup> (AFM). Resonating cantilevers are a very promising type of mass-sensitive chemical sensor<sup>20–22</sup>, especially if properly co-integrated with circuitry<sup>23</sup>. The absorption of analyte in the chemically sensitive polymer causes shifts in resonance frequency as a consequence of changes in the oscillating mass (Fig. 1b). Our CMOS resonant chemical sensor is based on a 150- $\mu\text{m}$ -long cantilever, which consists mainly of silicon, with some vapour-deposited oxide and thermal oxide. The different thermal expansion coefficients of the silicon and the oxide (bimorph effect) are used to initiate a cantilever vibration by periodically applying electric pulses to heating resistors embedded at the cantilever base. The cantilevers resonate at their fundamental mechanical frequency of 380 kHz with a quality factor of approximately 1,000 in air. The cantilever vibration is detected by embedded piezoresistors in a Wheatstone-bridge configuration. An on-chip low-noise fully differential difference amplifier with a gain of 30 dB amplifies the output signal of the Wheatstone bridge. The cantilever acts as the frequency-determining element in a feedback oscillation circuit, which was (for the first time, to our knowledge) entirely integrated on the chip with a counter. For more details on the electronics, see ref. 23.

The third transducer is a thermoelectric calorimeter based on the Seebeck effect, which detects enthalpy changes on absorption (heat of condensation) or desorption (heat of vaporization) of analyte molecules in the polymer film<sup>24,25</sup> (Fig. 1c). These enthalpy changes cause temperature variations on thermally insulated micromachined membranes. An array of 256 polysilicon/aluminium thermocouples connected in series is sandwiched in between the dielectric membrane layers to record these temperature variations. Their hot junctions are located on the membrane, the cold junctions

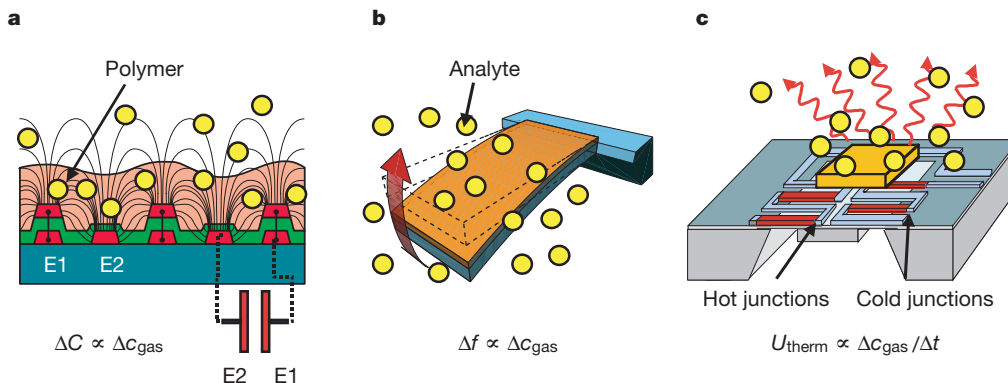


**Figure 1** Principles of three different types of transducer. **a**, Microcapacitor sensitive to changes in dielectric properties (capacitance change,  $\Delta C$ , proportional to analyte concentration change,  $\Delta C_{\text{gas}}$ ); **b**, resonant cantilever sensitive to mass changes (frequency change,  $\Delta f$ , proportional to analyte concentration change,  $\Delta C_{\text{gas}}$ ); and

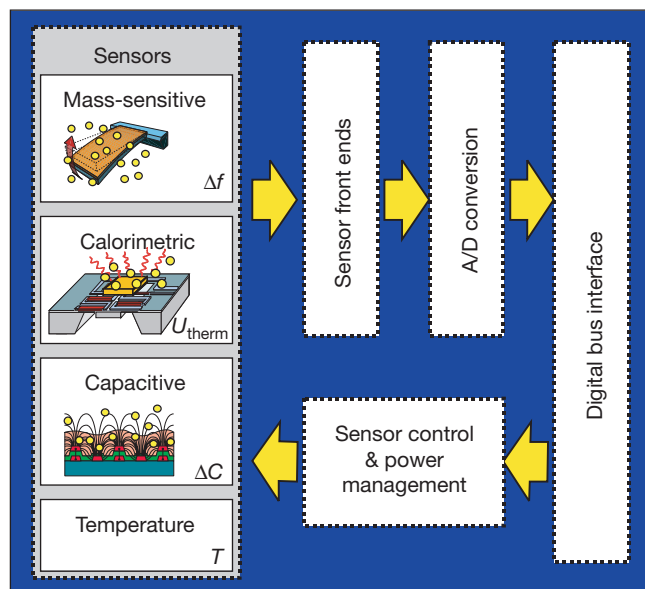


**Figure 2** Diagram of the overall microsystem architecture. It consists of sensors, driving and signal-conditioning circuitry (sensor front end), analog-to-digital converters, sensor control and power management unit, and a digital interface.

on the bulk chip. A thermovoltage between the hot and cold junctions develops, which is proportional to the temperature difference (in the millikelvin range). The calorimetric sensing process thus includes four principal steps: (1) absorption of the analyte and subsequent partitioning, (2) liberation or abstraction of heat, which causes (3) temperature changes, which are (4) transformed into thermovoltage changes<sup>26,27</sup>. In contrast to the capacitive and gravimetric chemical sensors relying on equilibrium signals, the calorimetric sensor detects only transients, meaning only changes in the analyte concentration<sup>24–27</sup>.

The calorimetric sensor system includes two  $500 \times 500 \mu\text{m}$  dielectric membranes, one of which is coated with the gas-sensitive polymer, while the other is left uncoated and serves as a reference<sup>28</sup>. The sensing and reference thermopiles are connected in parallel to the input stage of a low-noise, chopper-stabilized, instrumentation amplifier on-chip (gain 8,000, bandwidth 500 Hz) to record the temperature differences between the two membranes. The thermovoltage is translated into a digital signal on-chip using a sigma-delta analog-to-digital converter and a decimation filter.

The overall system chip also includes a temperature sensor,

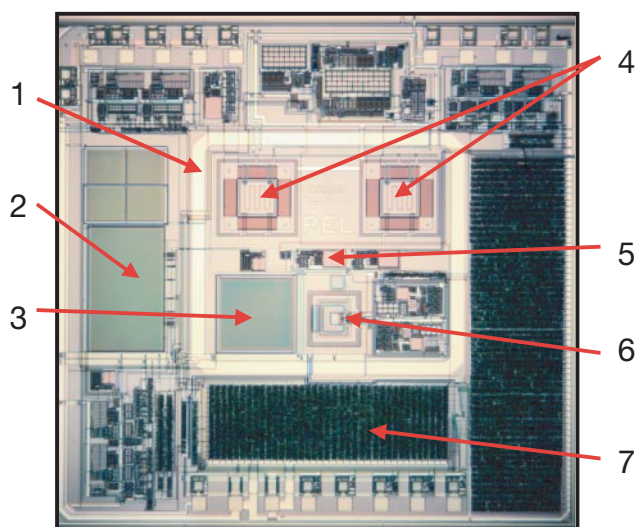


**Figure 3** Micrograph of the gas microsensor system chip (size,  $7 \times 7$  mm). The different components include: 1, flip-chip frame; 2, reference capacitor; 3, sensing capacitor; 4, calorimetric sensor and reference; 5, temperature sensor; 6, mass-sensitive resonant cantilever; and 7, digital interface.

because bulk physisorption of volatiles in polymers is strongly temperature-dependent: a temperature increase of  $10^\circ\text{C}$  decreases the fraction of absorbed analyte molecules by approximately 50%, and thus leads to a drastic sensor signal reduction. The operation temperature must be exactly known to enable quantitative measurements. The temperature sensor relies on the linear temperature dependence of a bipolar transistor available in the CMOS process. The voltage is converted to a digital signal using a sigma-delta converter. After calibration, the temperature sensor exhibits an accuracy of  $0.1\text{ K}$  at operation temperatures between  $223$  and  $383\text{ K}$ .

A diagram of the overall microsensor system architecture is shown in Fig. 2, and a chip micrograph is displayed in Fig. 3. On the left-hand side of Fig. 2, we have the four different sensors. The sensor front ends represent all the sensor-specific driving circuitry and signal-conditioning circuitry, as already described in the context of the different transducers. The analog-to-digital conversion is done on-chip as well. This leads to a high signal-to-noise ratio, because noisy connections are avoided and a robust digital signal is generated on-chip and then transmitted to an off-chip data port via an I<sup>2</sup>C digital interface (I<sup>2</sup>C is a communication standard developed by Philips, Eindhoven, The Netherlands). The I<sup>2</sup>C bus interface

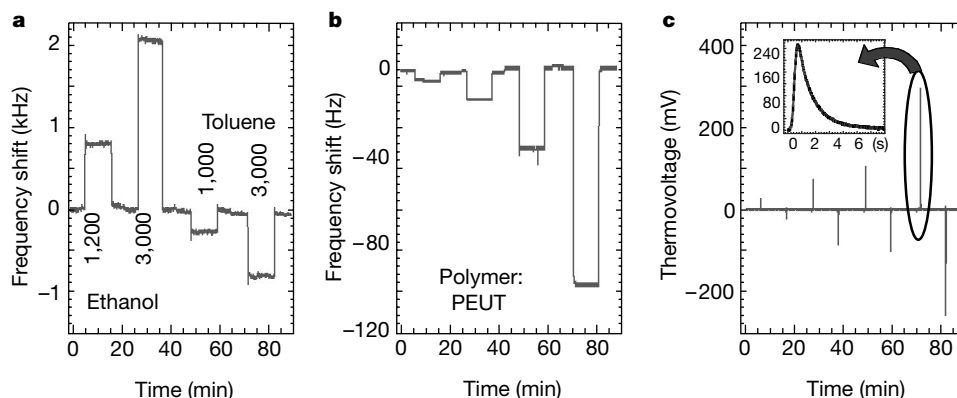
offers the additional advantage of having only very few signal lines (essentially two) for bi-directional communication, and also allows the operation of multiple chips on the same bus system. An on-chip digital controller manages the sensor timing and the chip power budget.

Figure 3 shows the processed and tested single-chip gas sensor system. The overall chip size is  $7 \times 7$  mm. The chip processing steps include an unaltered 15-mask commercial CMOS process (provided by austriamicrosystems, Unterpremstätten, Austria), followed by the application of a back-side mask and anisotropic potassium hydroxide etching of the membrane structures for the calorimetric sensors and the cantilever. Front-side reactive ion etching is then applied to release the cantilever from the respective membrane. Finally, the cantilever, calorimeter and capacitor sensors are coated with the polymer using an airbrush method. The sensors are located in the centre of a metal frame, which is used to apply a flip-chip packaging technique<sup>29</sup>.

Figure 4 displays simultaneously recorded sensor signals of the three transducers upon exposure to  $1,200$  and  $3,000$  p.p.m. of ethanol, and  $1,000$  and  $3,000$  p.p.m. of toluene, at  $301\text{ K}$ . The sensors were alternately exposed to analyte-loaded gas and pure carrier gas. The polymeric coating consisted of poly(etherurethane)<sup>27</sup>, at a thickness of approximately  $4\ \mu\text{m}$ . Figure 4a shows the measured frequency signals (output of the sigma-delta converter) of the capacitor. Ethanol—with a dielectric constant of  $24.5$ , which is larger than that of poly(etherurethane) ( $2.9$ )—causes a capacitance increase and hence positive frequency shifts, and toluene (with a dielectric constant of  $2.4$ ) causes a capacitance decrease and hence negative frequency shifts. The limits of detection are  $3$ – $5$  p.p.m. for ethanol and  $5$ – $8$  p.p.m. for toluene.

Figure 4b displays the cantilever response. Ethanol shows rather low signals as compared to toluene, owing to its lower molecular mass and its lower enrichment (partitioning) in the polymeric phase. The extent of physisorption is, to first order, inversely proportional to the boiling temperature of the analyte (ethanol,  $351\text{ K}$ ; toluene,  $360\text{ K}$ ): the lower the boiling temperature, the less enrichment in the polymer<sup>13</sup>. Here, the limits of detection are  $10$ – $12$  p.p.m. for ethanol and  $1$ – $2$  p.p.m. for toluene, which is comparable to other mass-sensitive transducers<sup>30</sup>.

The calorimetric results in Fig. 4c represent a superposition of already discussed partitioning and heat-budget change due to analyte ab/desorption. The absorbing analyte liberates heat (predominantly heat of condensation) causing a positive transient signal (positive peak), whereas the desorbing analyte abstracts vaporization heat from the environment, generating a negative transient signal (negative peak upon purging, see Fig. 4c). The inset in Fig. 4c shows the time-resolved response during the first six seconds of



**Figure 4** Sensor signals simultaneously recorded from all three polymer-coated (poly(etherurethane), PEUT) transducers. The transducers were exposed to  $1,200$  and  $3,000$  p.p.m. of ethanol, and  $1,000$  and  $3,000$  p.p.m. of toluene, all at  $301\text{ K}$ . **a**, Frequency shifts (Sigma-Delta converter output) of the capacitor; **b**, frequency shifts of

the resonating cantilever; and **c**, thermovoltage transients of the calorimetric sensor. The inset in **c** is an expanded-scale view, showing the development of the calorimetric transient within  $6\text{ s}$ .

exposure to 3,000 p.p.m.. The condensation/vaporization heat of ethanol is larger than that of toluene (42.3 compared to 38.0 kJ mol<sup>-1</sup> at 298 K) owing to directional interaction in the liquid phase (compare, for example, water), whereas the polymer partitioning of toluene is stronger owing to its higher boiling point. The limits of detection of the calorimetric method are larger than those of the other transducers (40–50 p.p.m. toluene, 100–150 p.p.m. ethanol).

The signals of all three transducers linearly correlate with analyte concentration at low concentrations (less than 3% of saturation vapour pressure at the operating temperature)<sup>13</sup>. As can be seen from the considerable variation in the transducer responses upon gas exposure, different molecular properties or different aspects of the coating–molecule interaction are measured by the different transducers. Alcohols, for example, provide comparably low signals on mass-sensitive transducers owing to their high saturation vapour pressure and low molecular mass, but provide large signals on capacitors owing to their large dielectric constant (24.5). Drastic changes in thermovoltages on the thermopiles are measured for chlorinated hydrocarbons (not shown here) used, for example, in cooling sprays, which in turn have a low dielectric constant, thus showing only small signals on capacitors.

Another powerful feature of the system is that even a zero response from one of the transducers, if there is a measurable response from the other two, is a highly informative data point to help identify the chemical species. To further improve analyte identification/quantification, an array of microsystem chips coated with different polymers could be used.

Our monolithic CMOS gas microsystem is intended to identify organic solvents in transport containers, or to provide information on workplace safety—in, for example, the chemical industry. It will form part of a hand-held or credit-card-sized detection unit. The CMOS approach offers substantial advantages, such as full microelectronics compatibility, extremely small size, low power consumption, and production at industrial standards. We expect that further research and the fast progress of microelectronics development will improve the device performance in the near future. □

Received 22 May; accepted 10 September 2001.

1. Massart, D. L., Vandeginste, B. G. M., Deming, S. N., Michotte, Y. & Kaufman, L. *Chemometrics: a Textbook* Vol. 2 (Data Handling in Science and Technology, Elsevier, Amsterdam, 1988).
2. Brereton, R. G. (ed.) *Multivariate Pattern Recognition in Chemometrics* Vol. 9 (Data Handling in Science and Technology, Elsevier, Amsterdam, 1992).
3. Hierlemann, A. et al. in *Sensors Update* Vol. 2 (eds Baltes, H., Göpel, W. & Hesse, J.) 119–180 (VCH, Weinheim, 1996).
4. Snow, A. W., Barger, W. R., Klusty, M., Wohltjen, H. & Jarvis, N. L. Simultaneous electrical-conductivity and piezoelectric mass measurements on iodine-doped phthalocyanine Langmuir-Blodgett films. *Langmuir* **2**(4), 513–519 (1986).
5. Rodriguez, J. L., Hughes, R. C., Corbett, W. T. & McWhorter, P. J. in *Technical Digest IEEE International Electron Devices Meeting* 521–524 (IEEE, New York, 1992).
6. Gumbrecht, W. et al. Integrated pO<sub>2</sub>, pCO<sub>2</sub>, pH sensor system for online blood monitoring. *Sensors Actuators B* **18–19**, 704–708 (1994).
7. Van den Berg, A., van der Waal, P. D., van der Schoot, B. B. & de Rooij, N. F. Silicon-based chemical sensors and chemical analysis systems. *Sensors Materials* **6**, 23–43 (1994).
8. Müller, G., Deimel, P. P., Hellmich, W. & Wagner, C. Sensor fabrication using thin-film-on-silicon approaches. *Thin Solid Films* **296**, 157–163 (1997).
9. Kovacs, G. T. A. *Micromachined Transducers* (WCB McGraw-Hill, Boston, 1998).
10. Madou, M. *Fundamentals of Microfabrication* (CRC, Boca Raton, Florida, 1997).
11. Suehle, J. S., Cavicchi, R. E., Gaitan, M. & Semancik, S. Tin oxide gas sensor fabricated using CMOS micro-hotplates and *in-situ* processing. *IEEE Electron Device Lett.* **14**, 118–120 (1993).
12. Vellekoop, M. J., Lubking, G. W., Sarro, P. M. & Venema, A. Integrated-circuit-compatible design and technology of acoustic-wave-based microsensors. *Sens. Actuators A* **44**, 249–263 (1994).
13. Hierlemann, A., Ricco, A. J., Bodenhofer, K., Dominik, A. & Göpel, W. Conferring selectivity to chemical sensors via polymer side-chain selection: Thermodynamics of vapor sorption by a set of polysiloxanes on thickness-shear mode resonators. *Anal. Chem.* **72**, 3696–3708 (2000).
14. Koll, A., Kummer, A., Brand, O. & Baltes, H. Discrimination of volatile organic compounds using CMOS capacitive chemical microsensors with thickness-adjusted polymer coating. *Proc. SPIE Smart Struct. Mater.* **3673**, 308–317 (1999).
15. Steiner, F. P. et al. in *Digest 8th Int. Conf. on Solid-state Sensors and Actuators* Vol. 2, 814–817 (Foundation for Sensor and Actuator Technology, Stockholm, 1995).
16. Gimzewski, J. K., Gerber, C., Meyer, E. & Schlittler, R. R. Observation of a chemical reaction using a micromechanical sensor. *Chem. Phys. Lett.* **217**, 589–594 (1994).
17. Stowe, T. D. et al. Attonewton force detection using ultrathin silicon cantilevers. *Appl. Phys. Lett.* **71**, 288–290 (1997).
18. Lange, D. et al. in *Proc. IEEE Workshop on Micro Electro Mechanical Systems (MEMS 99)* 447–452 (IEEE, Piscataway, 1999).

19. Chen, G. Y., Thundat, T., Wachter, E. A. & Warmack, R. J. Adsorption-induced surface stress and its effects on resonance frequency of microcantilevers. *J. Appl. Phys.* **77**, 3618–3622 (1995).
20. Thundat, T., Chen, G. Y., Warmack, R. J., Allison, D. P. & Wachter, E. A. Vapor detection using resonating microcantilevers. *Anal. Chem.* **67**, 519–521 (1995).
21. Lang, H. P. et al. A chemical sensor based on a micromechanical cantilever array for the identification of gases. *Appl. Phys. A* **66**, 61–64 (1998).
22. Maute, M. et al. Detection of volatile organic compounds with polymer-coated cantilevers. *Sensors Actuators B* **58**, 505–511 (1999).
23. Hagleitner, C., Lange, D., Brand, O., Hierlemann, A. & Baltes, H. in *Digest of Technical Papers IEEE International Solid State Circuits Conf. San Francisco* (ed. Wuorinen, J. H.) Vol. 44, 246 (IEEE, Piscataway, 2001).
24. Bataillard, P., Steffgen, E., Haemmerli, S., Manz, A. & Widmer, H. M. An integrated silicon thermopile as biosensor for the thermal monitoring of glucose, urea and penicillin. *Biosensors Bioelectron.* **8**, 89–98 (1993).
25. Lerchner, J., Seidel, J., Wolf, G. & Weber, E. Calorimetric detection of organic vapors using inclusion reactions with organic coating materials. *Sensors Actuators B* **32**, 71–75 (1996).
26. Van Heerwarden, A. W., Sarro, P. M., Gardner, J. W. & Bataillard, P. Liquid and gas micro-calorimeters for (bio)chemical measurements. *Sensors Actuators A* **43**, 24–30 (1994).
27. Hierlemann, A. et al. Application-specific sensor systems based on CMOS chemical microsensors. *Sensors Actuators B* **70**, 2–11 (2000).
28. Koll, A. et al. in *Proc. IEEE Workshop on Micro Electro Mechanical Systems (MEMS 99)* 547–551 (IEEE, Piscataway, 1999).
29. Koll, A. et al. A flip-chip-packaged CMOS chemical microsystem for detection of volatile organic compounds. *Proc. SPIE Smart Struct. Mater.* **3328**, 223–232 (1998).
30. Ballantine, D. S. et al. *Acoustic Wave Sensors: Theory, Design, and Physico-chemical Applications* (Academic, San Diego, 1997).

## Acknowledgements

We acknowledge the contributions of former staff of the Physical Electronics Laboratory at ETH Zurich who were involved in the development of the chemical microsensor. We also thank the prototype manufacturers austriamicrosystems for their services. This work formed part of a cooperative project involving the University of Tübingen (U. Weimar), the University of Bologna (M. Rudan), and ETH Zürich, which is financially supported by the Körber Foundation, Hamburg, Germany.

Correspondence and requests for materials should be addressed to A.H. (e-mail: hierlema@iqe.phys.ethz.ch).